EARTH SURFACE PROCESSES AND LANDFORMS, VOL. 21, 875–892 (1996)

GEOMORPHOLOGY AND KINEMATICS OF THE CONTURRANA ROCKSLIDE-DEBRIS FLOW (NW SICILY)

PIER GIORGIO NICOLETTI

CNR – IRPI, Via Verdi 248, 87030 Roges di Rende CS, Italy

AND

MARIO PARISE

CNR – CERIST, Via E. Orabona 4, 70125 Bari, Italy

Received 17 May 1994
Accepted 29 June 1995

ABSTRACT

The Conturrana rockslide-debris flow involved a mass of almost 22×10^6 m^3 of well indurated breccia with a plastic basal layer. The original rock mass slid initially along a listric slip surface – which required the rupture of the mass itself by internal shearing and caused the formation of a horst-and-graben morphology – and attained a high speed. Then part of the mass fell from a morphological step, and moved about 800 m forward. In this landslide, the morphological and morphometrical examination – which is also based on a reconstruction of the pre-landslide topography – indicates that mobility was rather low when related to volume and to the control exerted by local morphology. The event might have been induced by an earthquake in the 4th century.

KEY WORDS rockslide-debris flow; rockslide kinematics; geomorphic control; Sicily

INTRODUCTION

The rockslide-debris flow that took place on 28 July 1987 in Valtellina (Central Italian Alps) demonstrated once more how dangerous these landslides are: 29 people were killed, a permanent blockage was emplaced across an important river and economical losses were very heavy (Völk, 1989; Costa, 1991; Azzoni *et al.*, 1992). Unfortunately, our ability to tackle both the scientific and hazard-management problems posed by these landslides is still very limited. It is a widely held opinion that the study of cases which have already occurred is an essential part of the effort aimed at preventing risks from similar phenomena, and this work on the Conturrana rockslide-debris flow contributes to such an effort.

Although other, more concise terms are available in the literature to designate rockfall- and rockslide-debris flows, for the event of Conturrana the longer, but more descriptive, composite term (Varnes, 1978; IAEG Commission on Landslides, 1990) is particularly appropriate. There, in fact, a clearcut distinction is possible between the two stages.

The geology, morphology, morphometry and kinematics of this old landslide that started as a fast rockslide and evolved into a debris flow are dealt with in this article, as well as a reconstruction of the pre-landslide topography. The problems of dating and final trigger of the landslide will also be briefly treated. Although mentioned in non-scientific literature and sketched out in Agnesi *et al.* (1989), this landslide had never been specifically investigated hitherto.

CCC 0197-9337/96/100875–18

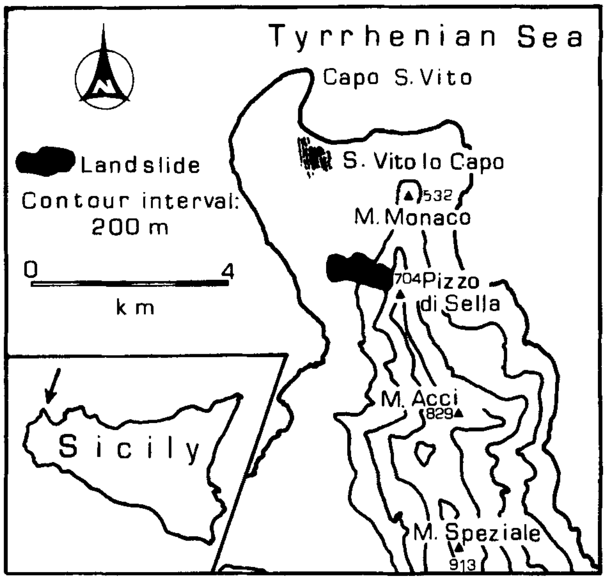

Figure 1. Schematic map of the study area and its surroundings

GEOLOGY AND SEISMICITY OF THE AREA

The Conturrana rockslide-debris flow is located on the western side of the Capo San Vito (Cape St. Vito) peninsula of NW Sicily (Figure 1), about 2 km south of the little town of San Vito lo Capo.

The Capo San Vito peninsula is formed by a NNW trending chain of fairly rugged mountains that consist mostly of carbonate rocks and attain a maximum elevation of 913 m. The rockslide took place on the western flank of Pizzo di Sella (Sella Peak), where part of the mass is still resting. The debris-flow deposit, about 800 m long, lies mostly on a nearly horizontal erosional surface formed probably in the lower Pleistocene (Agnesi *et al.*, 1989).

At present, mean annual rainfall in the area is 504 mm (Caloiero, 1975), which is low even for Sicily. Eighty per cent of this falls between September and February. There is no information as regards rainfall in the historical past.

Geology

The geological survey of the Capo San Vito peninsula by Giunta and Liguori (1970) forms, with modifications, the basis of the following description of the study area (Figure 2).

The outcropping formations belong to two tectono-stratigraphic units of the complex nappe structure of W. Sicily (Giunta and Liguori, 1972). The two units are separated by an overthrust surface and an exotic terrane (Plastic Complex). From the base upwards the following are encountered.

(1) *Lower tectono-stratigraphic unit*: (1a) Formation 'Calcare Pararecifale' (Parareefoid Limestone (PL); Cretaceous). This limestome is fine- to very fine-grained, strong to very strong, and thickly bedded to massive.
(2) *Overthrust surface*. Mean attitude is 180°/20°. Displacement along the overthrust occurred in late Miocene.
(3) *Formation 'Complesso Plastico'* (Plastic Complex (PC); middle to late Miocene). This has played a key role in the development of the landslide. The PC formation is a chaotic association of clastic rocks, and is perhaps reversed. It consists above all of poorly sorted, clayey-silty, and locally also sandy, material (Table I). Traces of bedding are usually rare and discontinuous. A 6–7 m thick bed of

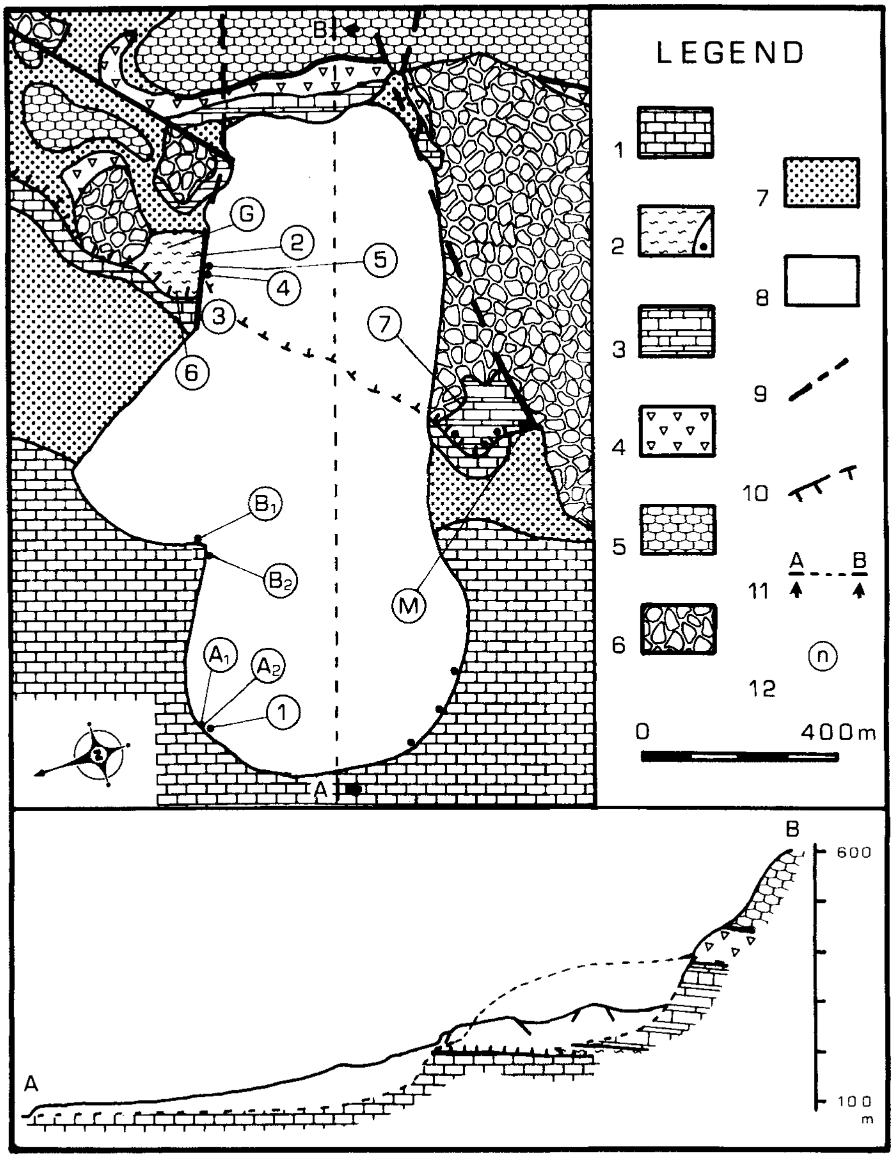

Figure 2. Geological map. Legend: (1) Parareefoid Limestone (PL). (2) Plastic Complex (PC). Single black dots indicate unmappable PC exposures. (3) Marly Limestone and Limestone (ML&L). (4) Radiolarite (R). (5) White and Red Algal Limestone (AL). (6) Breccia of Limestone Fragments (BLF). (7) Recent Debris (RD). (8) Landslide debris (mostly consisting of shattered BLF). (9) Faults, dashed where uncertain. (10) Overthrust. (11) Trace of section. (12) Sites of sampling of PC material, and other important places or features (see text for details). Section shows also the pre-landslide slope profile (dashed)

coarse-grained sandstone crops out in the quarry area (site 3 in Figure 2) on the northern side of the landslide. Obviously, rock material strength differs from member to member.

This complex is about 50 m thick N of the landslide, while S of it there are only a few scattered and unmappable exposures. Prior to the landslide it probably tapered with a certain continuity from N to S, and this difference in thickness must have influenced the morphology of the debris-flow deposit (see later on).

Small amounts of material originally belonging to this complex can be seen, completely remoulded, at several places along the distal rim of the debris flow, and were also encountered in an excavation at about 7–8 m below the deposit surface (site 1 in Figure 2).

Table I. Samples from the plastic complex

Grain-size distribution envelope	Sample code	Clay (%)	Silt (%)	Sand (%)	Specific weight ($g\,cm^{-3}$)	W_l (%)	W_p (%)	PI
	4	25	27	48	2·68	36·80	21·17	15·63
α	B1	19	32	49	2·68	39·70	28·22	11·48
	M	28	38	34	2·74	40·15	23·50	16·65
	1	39	42	19	2·57	50·00	23·37	26·63
	2	57	27	16	2·61	54·40	24·08	30·32
	5	43	51	6	2·56	33·40	19·32	14·08
β	A1	52	39	9	2·64	58·75	27·22	31·53
	A2	46	33	21	2·56	55.25	25.50	29·75
	B2	50	43	7	2·57	55·20	27·01	28·19
	G	66	24	10	2·74	59·81	30·89	28·92

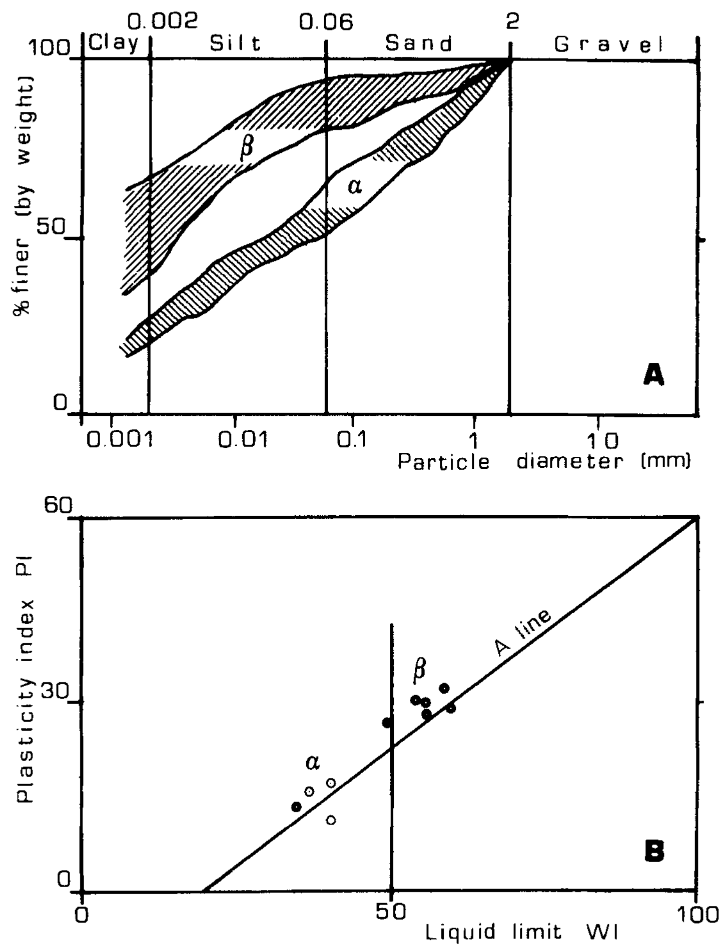

Figure 3. (A) Grain-size distribution envelopes and (B) plasticity chart for ten samples of PC soils from the landslide and its surroundings. In both diagrams the materials examined tend to form two different groups (α and β)

Figure 4. A typical aspect of the Breccia of Limestone Fragments, here exposed in a recent cut. Fence posts are about 2 m high

Grain-size distribution analyses and Atterberg limits were performed on ten samples from this formation (Figure 3 and Table I). All samples were collected at the surface and are remoulded; sampling points are shown in Figure 2, distinguished by their respective codes. The following results were obtained.

(a) Clay and silt represent more than half the weight of each sample. In particular, for samples in the α grain-size distribution envelope, they represent 51 to 66 per cent of the weight, and for samples in the β envelope, 79 to 94 per cent.

(b) Average specific weight for samples in envelope α is $2{\cdot}61\,\mathrm{g\,cm^{-3}}$, and for samples in envelope β $2{\cdot}70\,\mathrm{g\,cm^{-3}}$.

(c) α samples and β samples plot in different fields in the plasticity chart.

Based on this limited evidence, it seems that soils of at least two types can be distinguished in the PC formation. Grain-size distribution and index properties of all soils, and of β materials in particular, do not seem to contrast with the role attributed to this formation to account for the development of the landslide.

(4) *Upper tectono-stratigraphic unit*: (4a) Formation 'Calcare marnoso e Calcare' (Marly Limestone and Limestone (ML&L); late Cretaceous). This consists of alternating thin, often undulated or contorted beds of marlstone and calcareous marlstone, and of limestone. The limestone layers are usually only a few centimeters thick, but occasionally attain a thickness even greater than 1 m. Rock strength is variable, depending on composition.

(4b) Formation 'Radiolarite' (Radiolarite (R); late Jurassic to early Cretaceous). This formation consists of undulated beds, from 1–2 to 20 cm thick, of calcilutite with abundant chert, of marlstone, and of cherty limestone. Rock strength is variable. This formation is in contact with the following by means of a thrust-fault surface.

(4c) Formation 'Calcare Bianco e Rosso Algale' (White and Red Algal Limestone (AL); early Jurassic). This consists of massively bedded, strong limestone. This rock forms a rather sharp crest at the top of the mountain.

Apart from the formations belonging to the nappe structure, two more formations can be defined, namely a well indurated *Breccia a Frammenti Calcarei* (Breccia of Limestone Fragments (BLF)), and a loose or almost loose *Detrito Recente* (Recent Debris (RD)).

The Breccia is extensively exposed both in the study area and its surroundings. More importantly, it forms almost all of the visible landslide debris. This Breccia (Figure 4) consists of mostly subangular, whitish to light greyish brown limestone fragments, ranging in size from blocks, some of which are several metres in

Table II. Structural data

Formation	Type of discontinuity	Dip direction/Dip (°)
Parareefoid Limestone (PL)	Joints	005 to 085/65 to 90
		210 to 260/60 to 90
	Joints	115 to 175/60 to 90
		270 to 340/40 to 90
	Bedding	210 to 220/5 to 20
	Minor fault	257/68
	Minor fault	176/80
	Minor fault	170/78
	Minor fault	154/56
	Minor fault	140/63
	Minor fault	144/75
	Minor fault	194/83
	Minor fault	025/65
Marly Limestone & Limestone (ML&L)	Joints	070 to 100/75 to 90
		250 to 280/70 to 90
	Joints	310 to 010/45 to 90
	Bedding	050 to 095/10 to 20
	Minor fault	169/67
	Minor fault	331/74
	Minor fault	352/65
	Minor fault	203/38
	Minor fault	019/66
	Minor fault	150/55
Algal Limestone (AL)	Joints	085 to 115/50 to 70
		260 to 280/70 to 80
	Minor fault	278/70
	Minor fault	130/60
	Minor fault	101/55
Breccia (BLF)	Joints	295 to 345/75 to 90
	Tension cracks	090 to 125/80 to 90

diameter, to coarse sand. Matrix content is variable, cement is light brownish red or, less frequently, whitish. Texture is frequently clast-supported, porosity is generally high. The rock is very well cemented and strong. Sometimes a faint normal grading can be seen. It is also possible to observe layers, up to 1 m thick, of honeycomb calcrete (Netterberg and Caiger, 1983). The BLF mantles wide areas, also on gently sloping terrain (NW of the landslide in Figure 2), and is even found, several metres thick, in the summit area (NW of the study area, out of figure). This formation is probably a megabreccia (Longwell, 1951), i.e. a breccia that is partly sedimentary and partly tectonic in origin.

Permeability of the BLF formation is high. Site 7 in Figure 2 is the location of a small spring at the BLF–ML&L contact. Other springs were probably existing along the contact between BLF and the much less permeable PC in the pre-landslide geological configuration.

As noted above, the landslide body consists of BLF, plus some PC in the basal part; rocks other than BLF and PC have been looked for but never found. Furthermore, in the steep main scarp of the landslide, isolated patches of Breccia can be seen still adhering to the ML&L with a lateral contact which is both abrupt and strongly cohesive. The overall impression is that the Breccia occupied a pre-existing half-bowl-shaped cavity.

The structural observations made in the field and from aerial photographs are summarized, respectively, in Table II and Figure 5. Exposures suitable for taking structural measurements are not numerous, are often

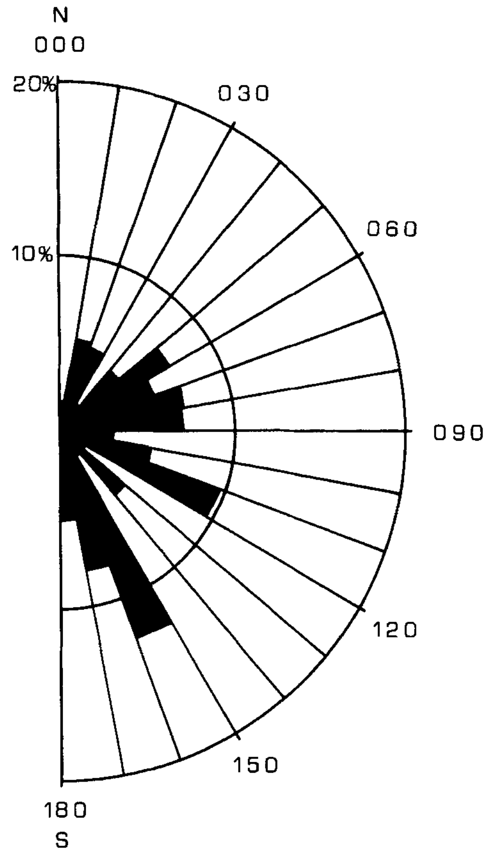

Figure 5. Rose diagram of lineaments as obtained from photointerpretation, expressed as percentage of cumulative length

N–S oriented and, with the exception of the PL formation, are generally difficult to reach. Therefore the data in the table cannot be considered as unbiased, and represent a partial picture of the real situation.

To the right of the landslide source, the surface of a normal left-slip fault, dipping about 200°/85°, cuts the lower unit and the PC, and may possibly be followed across the upper unit. Displacement of the S block is about 30 m downwards and an estimated 50 m eastwards. Another fault can be seen 200 m S of the landslide, where the attitude is 301°/65° and the N-side block is downthrown about 1·5 m. The supposed continuation of this fault may possibly be traced along part of the left side of the landslide source.

The resistant limestone of the lower unit forms a cliff 125 to 225 m above the erosional plain which is located at about 75 m a.s.l. This cliff is a prominent morphological step whose two ends appear as rock spurs at both sides of the landslide while its central part is buried by the debris. This landform (hereinafter called 'the cliff') marks the boundary between the rockslide and the debris flow.

Seismicity

Between AD 1000 and 1980 Sicily and the surrounding seas were hit by a number of earthquakes (Postpischl, 1985). Of these, 195 were of degree VII (MCS scale), 56 of degree VIII, 17 of degree IX, one of degree X, and three of degree XI. However, most of this activity occurred in eastern Sicily (Mt Etna and the Strait of Messina). In such a context, the Capo San Vito area appears to be weakly seismic: in fact, maximum epicentral intensity in the surrounding area reached no more than degree VII, and only two such earthquakes are recorded.

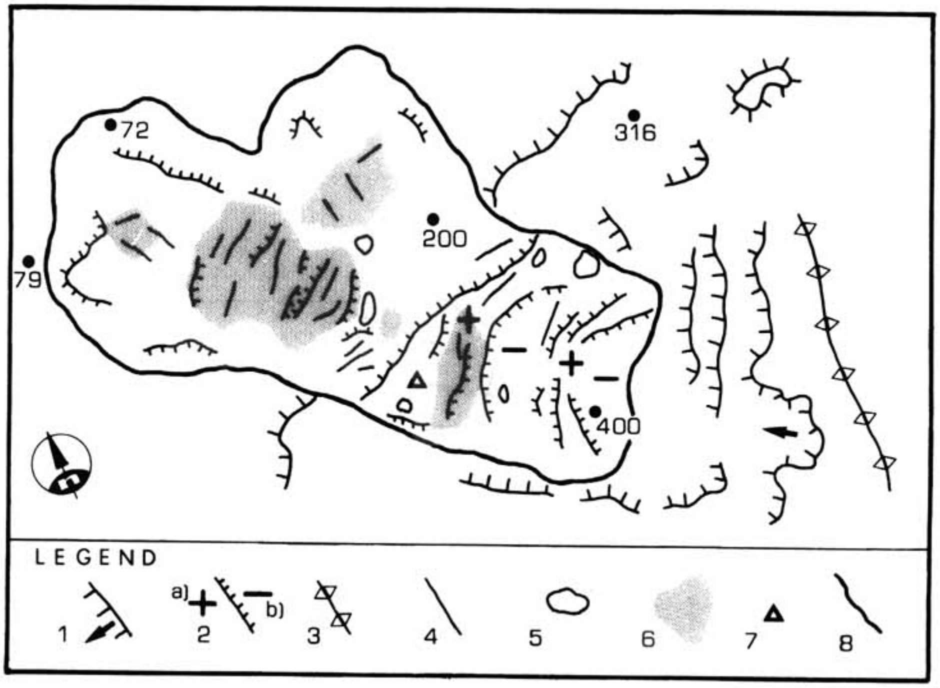

Figure 6. Morphological features of the landslide. This drawing is derived directly from photointerpretation, and is not to scale. Some elevations are given. Legend: (1) scarps external to the landslide – arrow indicates source and direction of the minor rockfall mentioned in the text; (2) scarps internal to the landslide with (a) horst-like and (b) graben-like features; (3) crest line of mountain; (4) cracks and crevasses; (5) depressions; (6) concentrations of blocks and boulders; (7) triangular, relatively undisturbed, plate; (8) landslide deposit boundary

As far as seismicity before AD 1000 is concerned, in spite of much recent progress in knowledge of the ancient seismic history of Italy and the Mediterranean area (Guidoboni, 1989), data concerning Sicily are still disappointingly scarce. Nevertheless, historical sources and archaeological evidence indicate that Sicily felt the destructive effects not only of local earthquakes, but also of some events with epicentres in N Africa or in the eastern Mediterranean area (Anonymous, 1989). Among these, those occurring between AD 306 and 310 (heavy damage in N Africa, damage in Sicily (Di Vita, 1982, 1990)), and those of AD 365 (probably several epicentres in eastern and central Mediterranean, with heavy damage reported in Greece, Palestine, Lybia and Sicily (Jacques and Bousquet, 1984; Guidoboni *et al.*, 1989; Di Vita, 1990)) are compatible with the time when, according to a local tradition, the landslide took place.

MORPHOLOGY AND PRE-LANDSLIDE TOPOGRAPHY

Morphology

The morphological features observed in the field and from aerial photographs are shown in Figure 6. The landslide deposit consists of two parts: the remnants of the rockslide mass, still resting upon the rupture surface above the cliff, and the debris-flow deposit, extending in front of and below the cliff. The ensuing description will basically follow this order, but a landform located uphill of the landslide will be dealt with first.

In the crest of Algal Limestone at the summit of the mountain, the source and part of the track of a relatively minor rockfall can be observed. The surface of the failed rock mass can be estimated at about 10 000 m^2, the thickness at a minimum of 20 m, and hence the volume is at least $0{\cdot}2 \times 10^6\ m^3$. Interestingly, the deposit of this rockfall is not visible at all, which means that it occurred prior to the main landslide. The

intriguing question of whether it occurred just prior to the main landslide, and therefore contributed to triggering it, must unfortunately remain unanswered.

The main landslide scarp is steeply inclined. At the base of the scarp a very steep talus is continuously fed by falling rocks.

The large depression at the base of the main scarp is about 25 m deep, and is limited downhill by a narrow crest which is concave uphill. A similar but smaller depression is located about 200 m downhill. These depressions and the interposed ridges create a typical horst-and-graben morphology. Other, less pronounced depressions can be seen along the flanks of the rockslide body.

Several features, such as scarps, crevasses and, above all, alignments of blocks, are concave uphill in plan view. Most of the scarps are almost transverse to the main direction of movement.

Just above the cliff, a relatively undisturbed area, triangular in shape and showing minor surface features, is evident on the S side of the rockslide.

The debris-flow deposit, downhill of the cliff, consists of a chaotic – but well delimited and internally continuous – heap of rock debris. In spite of the complete disruption of most of the material, blocky debris alignments and scarps are still evident. These are transverse to the main direction of movement, and are mainly concentrated in the southern part.

In the debris-flow deposit the surficial grain size of material decreases downhill, as is normal in these landslides (Abele, 1974). However, there is a rather sharp change below the 125–150 m altitude, which probably reflects some major variation in strength in the original rock mass.

Spreading of debris seems to have been more pronounced on the northern than on the southern side, probably because on the N side both the thickness of the basal PC layer and the height of fall were greater.

In addition, the N side presents a minor lobe, whose formation can probably be explained in the same way as the difference in spreading. The characteristics of this lobe do not differ from those described for the main lobe, and no shear surface can be observed between the two.

The geometric succession of the formations involved, Plastic Complex surmounted by Breccia, is preserved in the deposit.

Karstic microforms (Perna and Sauro, 1978), such as solution flutes and grooves, and lapiés potholes, are common at the surface of the blocks, and testify to the old age of the landslide.

Reconstruction of pre-landslide topography

Volume is a critical element in rockslide-debris flows, and has therefore to be estimated with accuracy. Taking dilatancy into account, the total volume of the deposit should correspond approximately to the volume of the original rock mass. It is also necessary to know the configuration of the original rock mass both for taking morphometrical measurements and for understanding the kinematics of the event. A reconstruction of the pre-landslide topography is therefore opportune (Figure 7).

As discussed by Abele (1974), reconstructing a pre-landslide topography is a puzzling, and sometimes impossible, task. Although many attempts have doubtless been made, only in a few cases have the results been published and analysed in some depth: examples are the Mt Granier rock avalanche (Goguel and Pachoud, 1972; Cruden and Antoine, 1984), the Usoy rockslide (Gaziev, 1984), the Slumgullion earthflow (Parise and Guzzi, 1992), the Waikaremoana landslide (Read *et al.*, 1992), and the Scanno rock avalanche (Nicoletti *et al.*, 1993).

In general, the reconstruction of a pre-landslide topography is subject to geological, morphological and mechanical constraints. Each of them is cross-checked against the others, so that the final picture is reasonably consistent. It has also to be assumed that all topographic variations occurring after the landslide are negligible.

At Conturrana the constraints are as follows.

(1) *Geological constraints*

(1a) Lithology of landslide deposit. Field evidence indicates that it consists mostly of Breccia, with a limited amount of Plastic Complex in the basal layer of the debris-flow deposit (it is unknown whether some PC is still present at the sole of the rockslide deposit).

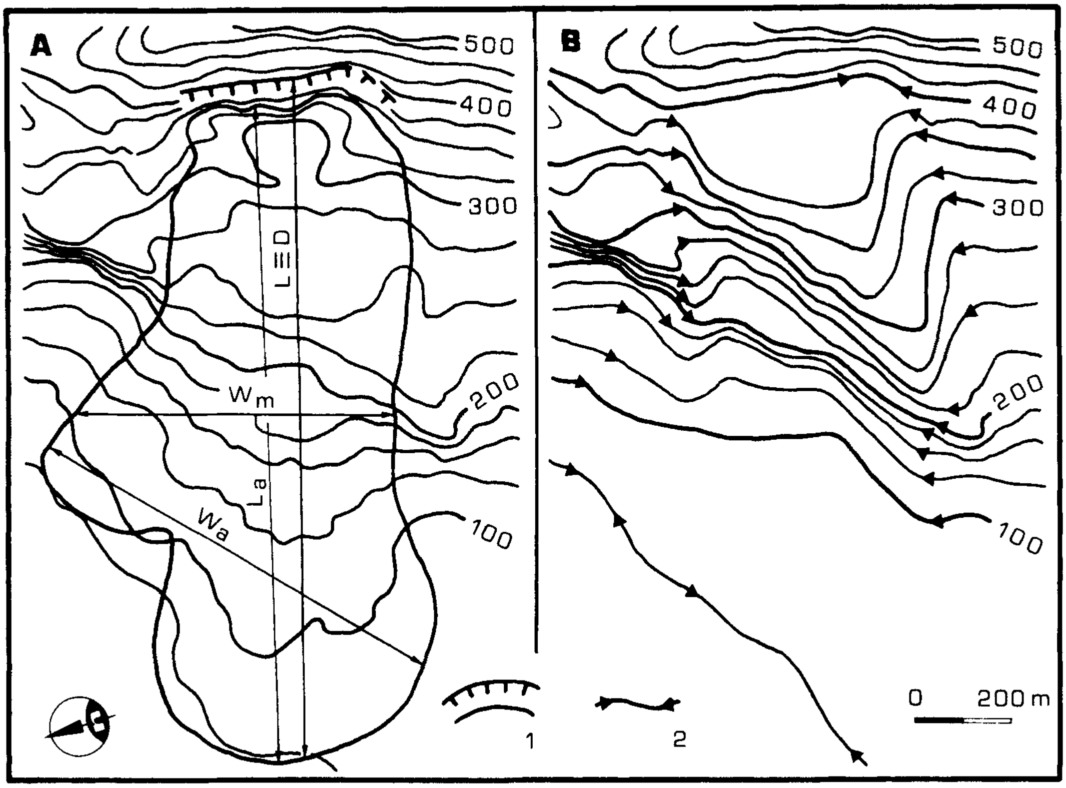

Figure 7. (A) Present topography of the landslide and its surroundings. Some important morphometrical parameters are also shown (see Table III for definitions). (B) Reconstructed pre-landslide topography. Legend: (1) main scarp, and landslide deposit boundary; (2) reconstructed parts of contour lines

(1b) Presence and attitude of the surface of the overthrust. Clearly, movement occurred along but not across this surface.

(1c) Presence and attitude of the faults along the two flanks of the rock mass. Here too, movement may have taken place along but hardly across these surfaces.

(1d) Continuity with the geological situation outside the landslide.

(2) *Morphological constraints*

(2a) The cliff in the PL formation, whose edge gradually descends from approximately 300 m on the right to 200 m on the left.

(2b) The roughly triangular plate of relatively undisturbed Breccia, that lies at about 250 m elevation (Figure 6). This plate must have been located somewhere in the pre-landslide topography.

(2c) Agreement of volumetric data.

(2d) The planimetric spacing of the 200 m and 300 m contour lines, which in present topography varies between about 200 m on the right and about 500 m on the left of the landslide source.

(2e) A small, presumably fault-controlled incision visible S of the landslide. Before the event, this incision probably continued upstream, within – or at the margin of – the mass that would fail.

(3) *Mechanical constraints*

(3a) Subdivision of the mass during the event. The horst-and-graben morphology visible in Figures 2 (section) and 6 indicates that the rock mass must have split into several parts. This usually happens when a rigid mass of rock has to follow a listric slip surface, which imposes severe shearing deformation (Skempton and Hutchinson, 1969; Rib and Ta Liang, 1978; Hutchinson, 1988).

(3b) Presence in the original slope of materials which differed widely in mechanical properties. The soft PC sandwiched between the much more resistant PL and BLF clearly represented a layer of weakness, through which failure would preferentially occur. This is the origin of the listric form of the slip surface.

By analysing all these constraints, their roles and interactions, it was possible to arrive at the contour-line interpolation which materializes the reconstructed pre-landslide topography. The resulting picture (Figure 7B) shows a bulging rock mass that is connected with the mountain slope almost only in its rear and lower parts: lateral restraint is little developed, thus determining a situation unfavourable to stability (Hoek and Bray, 1981). The basal support offered by the PL formation, which formed a platform protruding out of the slope in that site alone, undoubtedly gave a significant contribution to the development of this landform.

MORPHOMETRY AND GEOMORPHIC CONTROL OF THE LANDSLIDE

Morphometric data are listed in Table III, and only some comments are added here.

The total volume of deposit is 15 per cent greater than the volume of the original rock mass, as a result of the increase in porosity following fragmentation. However, in rockfall- and rockslide-debris flows the increase usually observed is of the order of 30 per cent. This discrepancy can be explained by considering that during the rockslide stage the material that was moving upon the concave and, presumably, rather smooth slip surface remained under some confining pressure. Leaving aside the deformation resulting in horst-and-graben morphology, it must therefore have suffered only little disruption (Hungr, 1981). Pronounced fragmentation, and therefore substantial volume increase, was necessarily limited to the debris-flow deposit. Calculations indicate that a volume increase of about 28 per cent occurred in the debris flow, and this fits the expected figure. With its debris volume of about $25 \times 10^6\,m^3$, the Conturrana rockslide-debris flow can be classified among the small events of this kind.

The elevation difference in this landslide is only 335 m, one of the lowest values recorded for such events.

This landslide is tongue-shaped overall, although the minor lobe deforms its northern side. After abandoning the cliff, the debris was able to move on a flat and almost level surface free from lateral confinement and to stop spontaneously (i.e. without expending energy in impacts with external obstacles). These characteristics denote that a moderate-energy-dissipative geomorphic control (Nicoletti and Sorriso-Valvo, 1991) acted on the landslide. The shape index W_m/W_a is very close to the average for landslides of this class. The values of W_m/D and W_a/D are unusually high, but this depends on the presence of the minor lobe which determines high values for both W_m and W_a. In this respect, this landslide compares well with those where – geomorphic control being equal – considerable lateral spreading of the deposit took place, namely Sasso Englar (Fuganti, 1969), Goldau (Heim, 1932), Frank (McConnell and Brock, 1904), Stalk Lakes and Maligne Lake (Mollard, 1977).

A distinctive feature of rockslide-debris flows is their mobility, i.e. the debris masses produced through the initial failure exhibit the capability of moving at high velocity for a long distance, also over gently inclined to flat ground (and sometimes also upslope). In each case, volume, characteristics of the travel path, and rheology of the debris mass determine the velocity, the distance travelled, and so on, i.e. how pronounced the mobility is. Clearly, for the complex landslide of Conturrana, mobility was mostly related to the behaviour of the mass in the debris flow.

Commonly, mobility is evaluated by plotting relevant parameters (such as the runout distance L, the excessive travel distance L_e, or the equivalent coefficient of friction H/L) versus volume. By doing this, it was found by comparison with similar events (Nicoletti and Sorriso-Valvo, 1991) that the mobility of the debris flow under examination was rather limited. The sloping angle of the deposit, about 11°, is rather high, which again indicates limited mobility.

Average thickness is moderately high and relative thickness is high; both are in good agreement with the spreading index, which is rather low (Abele, 1974). All this can be easily explained by the remarkably high value of the relative hollow and the high value of the ratio $(D/L)_{SH}$, both of which indicate the compact form

Table III. Morphometric data

Feature		References and notes
Planimetric surface of the original rock mass	$S_r = 0{\cdot}258\ km^2$	
Volume of the original rock mass	$V_r = 21{\cdot}9 \times 10^6\ m^3$	
Maximum thickness of the original rock mass	150 m	
Planimetric surface of rockslide deposit	$S_{d1} = 0{\cdot}231\ km^2$	
Planimetric surface of debris-flow deposit	$S_{d2} = 0{\cdot}480\ km^2$	
Total planimetric surface of deposit	$S_d = 0{\cdot}711\ km^2$	
Total planimetric surface of the landslide	$S = 0{\cdot}733\ km^2$	
Volume of rockslide deposit	$V_{d1} = 10{\cdot}5 \times 10^6\ m^3$	
Volume of rock available for the debris flow	$V_r - V_{d1} = 11{\cdot}4 \times 10^6\ m^3$	
Volume of debris-flow deposit	$V_{d2} = 14{\cdot}65 \times 10^6\ m^3$	
Volume increase in the debris flow	$V_{d2}/(V_r - V_{d1}) = 1{\cdot}285$	
Total debris volume	$V_d = 25{\cdot}15 \times 10^6\ m^3$	
V_d/V_r	1·15	
Runout	$L = 1370\ m$	L is the planimetric distance (see Fig. 7) between the topmost point of the main scarp and the farthest point of toe, measured following the approximate direction of motion. In this and similar cases D coincides with L, while it does not when a high angle impact with the opposite slope occurs. D is necessary in order to define some indices dealt with in the following (see Nicoletti and Sorriso-Valvo (1991) for further detail).
Length	$D = 1370\ m$	
Elevation difference	$H = 335\ m$	Measured between the two points that define L.
Excessive travel distance	$L_e = L - H/\tan 32° = 834\ m$	Hsü (1975)
Mobility index	$H/L = 0{\cdot}245$	
Mobility index	$L_e/L = 0{\cdot}609$	
Length of deposit	$L_a = 1330\ m$	Planimetric distance (see Fig. 7) between the topmost point of the deposit and the farthest point of toe, measured following the approximate direction of motion (Heim, 1932; Abele, 1974).
Slope angle of deposit	11° (19·5%)	Measured between the points that define L_a
Planimetric width at $D/2$	$W_m = 670\ m$	See Fig. 7
Maximum planimetric width of deposit	$W_a = 900\ m$	See Fig. 7
W_m/W_a	0·744	Nicoletti and Sorriso-Valvo (1991)
$W_m/L = W_m/D$	0·489	Nicoletti and Sorriso-Valvo (1991)
$W_a/L = W_a/D$	0·657	Nicoletti and Sorriso-Valvo (1991)
Maximum thickness of deposit	85 m	
Average thickness of deposit	$= V_d/S_d = 35{\cdot}4\ m$	
Relative thickness of deposit	$= (V_d/S_d)/\sqrt{S_d} = 0{\cdot}042$	Abele (1974)
Spreading	$S_d/S_r = 2{\cdot}756$	Abele (1974)
Relative hollow	0·878	Ratio between maximum hollow of the landslide source and its width, measured at the same elevation (Abele, 1974).

Table III continued

Feature		References and notes
$(D/L)_{SH}$	0·227	D and L here must not be confused with those dealt with in the note relative to runout. This index (SH is for Skempton & Hutchinson, 1969) relates the maximum depth of the rock mass to its maximum initial down-slope extent. It is usually $\leqslant 0{\cdot}1$ in translational slides, between 0·15 and 0·33 in rotational slides, and has intermediate values in compound slides (Hutchinson, 1988). For the compound slide treated here its value is therefore high.

of the original rock mass, and by the limited mobility that hindered spreading and, consequently, thinning. Average thickness is remarkable even when compared to the value expected by applying the Hungr (1981) statistical relationship:

$$\text{thickness} = 0{\cdot}05\, V_{\mathrm{d}}^{1/3}$$

which gives here:

$$\text{thickness} = 14{\cdot}6\,\mathrm{m}$$

i.e. less than half the observed value. The results for deposit surface area are much smaller than expected by using the statistical relationship, also by Hungr (1981):

$$S_{\mathrm{d}} = 20\, V_{\mathrm{d}}^{2/3}$$

which gives here:

$$S_{\mathrm{d}} = 1{\cdot}72\,\mathrm{km}^2$$

i.e. more than twice the observed figure.

DISCUSSION: KINEMATICS OF THE LANDSLIDE

According to computations, more than $11 \times 10^6\,\mathrm{m}^3$ of rock were involved in the debris flow, which is about 800 m long and lies mostly on a surface sloping about 2°. Had the material fallen from the cliff in the form of small rockfalls, a talus slope (much steeper than the actual deposit) would have been generated. Since no talus slope is present, it is reasonable to assume that $11 \times 10^6\,\mathrm{m}^3$ of rock abandoned the cliff in a single episode. This, of course, required a large amount of energy, which only a high rockslide velocity could have provided. The origin of this high velocity has then to be investigated.

Evidence indicates that the basal slip surface followed the contact between ML&L and Breccia in the upper part, and then either remained within the PC, or crossed the PC as far as the overthrust and coincided with this surface afterwards. As the contact between ML&L and Breccia seems well-endowed with cohesive strength, and as tectonic movements along the overthrust had ceased in late Miocene and recementation could well have occurred since, it is difficult to imagine that significant parts of the basal slip surface were at residual strength. As a matter of fact, the contact between PL and PC can be observed today just N of the landslide (site 6 in Figure 2), where it is marked by a layer of slightly clayey siltstone. This rock is weakly cemented, and turns to powder easily under finger pressure. On both flanks, where the slip surface coincided, at least partly, with fault surfaces, conditions of residual strength were more probable.

Thus, through cohesion and recementation, a degree of brittleness was very probably present in the potential slip surface. In any case, the listric shape it possessed determined a kinematically inadmissible mechanism, capable of keeping the mass in place even if the factor of safety along that surface had been somewhat smaller than 1. Therefore, for a major movement to occur, two conditions had to be fulfilled:

(1) a breaking up of the rock mass by internal shearing, which determined a kinematically admissable mechanism;
(2) a factor of safety at least temporarily smaller than 1 along the bounding slip surface.

The horst-and-graben morphology of the rockslide body indicates clearly that a failure of internal shears occurred. The brittleness of the BLF mass caused this to happen quickly. A kinematically admissible mechanism was thus suddenly created and, as the factor of safety along the slip surface had to be smaller than 1, the mass could be rapidly accelerated by the excess driving forces. In such circumstances it is rather typical that the landslide takes place as a single event, and that, if the sliding mass is characterized by high internal brittleness (as is the case with the well-lithified BLF), failure attains very high speed (Hutchinson, 1988).

Why the factor of safety along the bounding slip surface was below 1 when the internal failure of the rock mass took place, is a very interesting question which, both for the sake of brevity and because of its

unavoidably hypothetical nature, cannot be explored here. However, given the variety of actions it can exert on both rock and pore water, an earthquake is the simplest explanation.

Presumably perched groundwater pressures favoured failure. In fact, the BLF is porous and fractured, and undoubtedly conveyed water to the much less permeable PC. The possible influence of a rockfall from the crest of the mountain has already been mentioned. Finally, since the sole of the rupture surface was dipping into the mountain (Figure 2, section), it is possible that a minor collapse from the front of the rock mass unloaded its toe, thus favouring or even provoking the major failure (Hutchinson, 1984, 1987, 1988).

Other factors, such as the development of heat along the slip surface (Voight and Faust, 1982; Davis *et al.*, 1990; Nonveiller, 1992) or a rapid drop in residual shear strength as displacement rate increased (Lemos *et al.*, 1985; Hutchinson, 1995) cannot be excluded.

About half of the failed mass – consisting of PC in the basal part – was thus launched beyond the edge of the cliff, fell, and moved westwards. On touching the ground, the PC material undoubtedly underwent sudden, very strong undrained loading, which presumably resulted immediately in undrained shearing (Sassa, 1988). This, in practice, means that movement may have taken place largely through undrained shearing of the basal PC material. It is suggested that the process was similar to that in case C described by Sassa (1988, p. 40): 'Case C is the case where a higher pore pressure is inside the landslide mass and dissipates to the ground, so the pore pressure at the slip plane is affected by both the landslide mass and the ground'. Interestingly enough, in the case of Conturrana, pore pressure probably dissipated towards both the ground (karsified limestone) and the overlying Breccia. Sassa (1988) also noted that in his case C the distance travelled was not great. This mechanism, along with the limited height of fall, could well explain the scarce runout exhibited in the debris-flow stage of this landslide.

AGE AND TRIGGER OF THE LANDSLIDE

A popular tradition of religious origin says that an enormous landslide destroyed the hamlet of Conturrana at the time of Diocletian (AD 240–313, Roman emperor from AD 284 to 305). With some variations – a landslide, an earthquake, a tsunami, are all mentioned, either one at a time or variously combined – this story is presented by several authors between the 16th and 19th centuries (cf. Battaglia, 1975, for a partial summary). Also some 'warning signs' of an impending landslide are mentioned (Milone, 1870), but unfortunately without detail or reference. No written account older than the 16th century seems to exist.

The site has never been methodically investigated by archaeologists. However, many terracotta fragments were found a few years ago above the landslide under approximately 70 cm of soil. On examination they proved to be of late-Roman or Byzantine age (7th–9th century) (Mannino, 1993).

This may indicate that the landslide took place before the 7th–9th century and, if local legend can be relied upon, probably in the 3rd or 4th century. As seen earlier, historically documented earthquakes occurred in the 4th century, and in Sicily some meaningful archaeological evidence seems to be linked with those events:

(1) At Patti (NE coast of Sicily, 200 km E of Capo San Vito), a Roman villa was presumably destroyed in AD 306, rebuilt and again destroyed, probably in AD 365 (Voza, 1982).
(2) In Palermo (NW coast, 60 km E of the cape), damage is datable to 365 (Camerata-Scovazzo, 1975).
(3) At Marsala (W coast, 50 km SW of the cape), buildings collapsed probably due to an earthquake in 365 (Di Stefano, 1984); moreover, large rebuilding works can be dated to between 306 and 361 (Di Stefano, 1971).
(4) At Piazza Armerina (south-central Sicily, 160 km SE of the cape), a Roman villa was destroyed, probably due to an earthquake in the period 306–310; after rebuilding, the villa was again damaged, probably in 365 (Di Vita, 1972–73, 1982).

Note that the destruction of a well-built stone building requires a macroseismic intensity of at least degree IX (MCS scale), which is also sufficient for triggering landslides. Therefore, a correlation between these earthquakes and the landslide is doubtless possible.

CONCLUSIONS

A typical rockslide-debris flow took place at Conturrana, involving a mass of well-lithified and brittle breccia with a plastic basal layer. The rock mass was bounded by a surface of listric form in section, which determined a kinematically inadmissible mechanism. Therefore, even with a factor of safety somewhat smaller than 1 along the bounding slip surface, the mass could not start moving unless internal shearing had previously taken place. When this occurred, a kinematically admissible mechanism was quickly created and the rock mass could be accelerated by the excess driving forces, attaining high speed.

At a cliff on the slope, about half of the mass abandoned the slip surface and fell about 170 m. After impact, this debris was able to move forward for several hundred metres, probably by means of a mechanism of undrained loading–undrained shearing of the plastic basal layer. This stage of movement took place across a subhorizontal terrain, free from obstacles.

On analysing the morphometrical data, it can be concluded that the mobility of this rockslide-debris flow was limited, when related to its volume and to the control exerted by local morphology.

Popular legend places the landslide in the 3rd–4th century, and terracotta fragments found above the deposit date back to the 7th–9th century. A correlation with earthquakes that occurred in AD 306–310 and in AD 365 is certainly possible, but evidence is not conclusive.

ACKNOWLEDGEMENTS

We express our warm gratitude to all those who, in various ways, helped us in this study: V. Adragna (former director of Erice Public Library) and E. Battaglia (former mayor of San Vito lo Capo) for assistance in bibliographical research; G. Belluomini (University of Rome) for the radiocarbon dating of a wooden sample unfortunately too recent to be significant; T. Lucchesi (Sicily Regional Authority) for assistance in finding aerial photographs; G. Mannino (formerly at the Monuments and Fine Arts Service, Palermo) for examining the terracotta fragments; L. Militi (CNR–IRPI) for performing soil tests; S. Monacò, for lending the terracotta fragments; M. Cesarò and A. Vultaggio (Restaurant 'Alfredo', site 1 in Figure 2), and Pace Bros. (Quarry 'Contessa Marmi', site 3 in Figure 2), for permitting entrance to their properties; finally to the director M. Govi, and to G. Gullà and M. Sorriso-Valvo (all at CNR–IRPI) for critically reading the paper and providing valuable suggestions.

REFERENCES

Abele, G. 1974. *Bergstürze in den Alpen*, Wissenschaftliche Alpenvereinshefte, München, **25**, p. 230 [Italian translation by Nicoletti, P. G. 1990–1994. *Bergsturz nelle Alpi*, Rapporti Interni CNR–IRPI, Cosenza, **289, 290, 291, 298, 303, 304, 305, 359, 366, 409, 419, 425, 436, 437**].

Agnesi, V., Macaluso, T. and Ulzega, A. 1989. *Guida alle Escursioni (Penisola di Capo San Vito, Isole Egadi, Santa Ninfa)*, Dipartimento di Geologia e Geodesia dell' Università, Palermo, p. 93.

Anonymous 1989. 'Area mediterranea: catalogo', in Guidoboni, E. (Ed.), *I Terremoti Prima del Mille in Italia e nell'area Mediterranea*, Edizioni Storia Geofisica Ambiente, Bologna, 622–717.

Azzoni, A., Chiesa, S., Frassoni, A. and Govi, M. 1992. 'The Valpola landslide', *Engineering Geology*, **33**, 59–70.

Battaglia, E. 1975. *Il Santuario di San Vito Martire in San Vito lo Capo (Trapani)*, Tipografia EriGraf, Valderice, p. 35.

Caloiero, D. 1975. *Le Precipitazioni in Sicilia nel Cinquantennio 1921–1970*, CNR–IRPI, Cosenza, Geodata **5**, p. 29.

Camerata-Scovazzo, R. 1975. 'Nuove proposte sul grande mosaico di Piazza della Vittoria a Palermo', *Kokalos*, **21**, 231–273.

Costa, J. E. 1991. 'Nature, mechanics, and mitigation of the Val Pola Landslide, Valtellina, Italy, 1987–1988', *Zeitschrift für Geomorphologie, N. F.*, **35**, 15–38.

Cruden, D. M. and Antoine, P. 1984. 'The slide from Mt. Granier, Isere and Savoie, France, on November 24, 1248', *Proceedings of the 4th International Symposium on Landslides, Toronto*, **1**, 475–481.

Davis, R. O., Smith, R. and Salt, G. 1990. 'Pore fluid frictional heating and stability of creeping landslides', *International Journal for Numerical and Analytical Methods in Geomechanics*, **14**, 427–443.

Di Stefano, C. A. 1971. 'Marsala (Lilibeo): nuove scoperte archeologiche', *Sicilia Archeologica*, **14**, 41–48.

Di Stefano, C. A. 1984. 'Fase Romana Imperiale', in *Lilibeo: Testimonianze Archeologiche dal IV secolo a. C. al V secolo d. C.*, Regione Siciliana, Assessorato dei Beni Culturali ed Ambientali, 134–139.

Di Vita, A. 1972–1973. 'La villa di Piazza Armerina e l'arte musiva in Sicilia', *Kokalos*, **18/19**, 251–263.

Di Vita, A. 1982. 'Evidenza dei terremoti del 306–310 e del 365 in monumenti e scavi di Tunisia, Sicilia, Roma e Cirenaica', *Africa. Fouilles, Monuments et Collections Archeologiques en Tunisie*, **7–8**, 127–139.

Di Vita, A. 1990. 'Sismi, urbanistica e cronologia assoluta. Terremoti e urbanistica nelle città di Tripolitania fra il I secolo a. C. ed il IV d. C.', in *L'Afrique dans l'Occident Romain*, Actes du Colloque organisé par l'Ecole Française de Rome, Rome 1987, 426–494.

Fuganti, A. 1969. 'Studio geologico di sei grandi frane di roccia nella regione Trentino-Alto Adige', *Memorie del Museo Tridentino di Scienze Naturali*, **17** (3), 1–72.

Gaziev, E. 1984. 'Study of the Usoy landslide in Pamir', *Proceedings of the 4th International Symposium on Landslides, Toronto*, **1**, 511–515.

Giunta, G. and Liguori, V. 1970. 'Geologia della penisola di Capo San Vito (Sicilia nordoccidentale)', *Lavori dell'Istituto di Geologia dell'Università di Palermo*, **9**, p. 29.

Giunta, G. and Liguori, V. 1972. 'Geologia dell'estremità nord-occidentale della Sicilia', *Rivista Mineraria Siciliana*, **136–138**, 165–226.

Goguel, J. and Pachoud, A. 1972. 'Geologie et dynamique de l'ecroulement du Mont Granier, dans le Massif de Chartreuse, en novembre 1248', *Bulletin du Bureau de Recherches Géologique et Minière, 2nd series, sec. III*, **1**, 30–38.

Guidoboni, E. (Ed.) 1989. *I Terremoti Prima del Mille in Italia e nell'area Mediterranea*, Edizioni Storia Geofisica Ambiente, Bologna, p. 765.

Guidoboni, E., Ferrari, G. and Margottini, C. 1989. 'Una chiave di lettura per la sismicità antica: la ricerca dei "gemelli" del terremoto del 365 d.C.', in Guidoboni, E. (Ed.), *I Terremoti Prima del Mille in Italia e nell'area Mediterranea*, Edizioni Storia Geofisica Ambiente, Bologna, 552–574.

Heim, A. 1932. *Bergsturz und Menschenleben*, Fretz und Wasmuth, Zürich, p. 218 [English translation by Skermer, N. A. 1989. *Landslides and Human Lives*, BiTech Publishers, Vancouver, BC, p. 195].

Hoek, E. and Bray, J. W. 1981. *Rock Slope Engineering*, 3rd edn, The Institution of Mining and Metallurgy, London, p. 358.

Hsü, K. J. 1975. 'Catastrophic debris streams (Sturzstroms) generated by rockfalls', *Geological Society of America Bulletin*, **86**, 129–140.

Hungr, O. 1981. *Dynamics of Rock Avalanches and other Types of Slope Movements*, PhD thesis, University of Alberta, p. 506.

Hutchinson, J. N. 1984. 'An influence line approach to the stabilization of slopes by cuts and fills', *Canadian Geotechnical Journal*, **21**, 363–370.

Hutchinson, J. N. 1987. 'Mechanisms producing large displacements in landslides on pre-existing shears', *Memoir of the Geological Society of China*, **9**, 175–200.

Hutchinson, J. N. 1988. 'General report: Morphological and geotechnical parameters of landslides in relation to geology and hydrogeology', *Proceedings of the 5th International Symposium on Landslides, Lausanne*, A. A. Balkema, Rotterdam, **1**, 3–35.

Hutchinson, J. N. 1995. 'Keynote paper: Landslide hazard assessment', *Proceedings of the 6th International Symposium on Landslides, Christchurch*, A. A. Balkema, Rotterdam, **3**, 1805–1841.

IAEG Commission on Landslides 1990. 'Suggested nomenclature for landslides', *International Association of Engineering Geology Bulletin*, **41**, 13–16.

Jacques, F. and Bousquet, B. 1984. 'Le raz de marée du 21 julliet 365. Du cataclysme local à la catastrophe cosmique', *Mélanges de l'Ecole Française de Rome, Antiquité*, **96** (1), 423–461.

Lemos, L., Skempton, A. W. and Vaughan, P. R. 1985. 'Earthquake loading of shear surfaces in slopes', *Proceedings of the 11th International Conference on Soil Mechanics and Foundation Engineering, San Francisco*, **4**, 1955–1958.

Longwell, C. R. 1951. 'Megabreccia developed downslope from large faults', *American Journal of Science*, **249**, 343–355.

Mannino, G. 1993. *Frammenti di Terracotta dalla Frana di Conturrana*, unpublished report, p. 2.

McConnell, R. G. and Brock, R. W. 1904. 'Report on the great rockslide at Frank, Alberta, Canada', *Canada Department of the Interior, Annual Report, 1902–1903, part 8*, p. 17.

Milone, C. 1870. *Gli Atti ed il Culto di San Vito Martire*, Uffizio delle Letture Cattoliche, Napoli.

Mollard, J. D. 1977. 'Regional landslide types in Canada', in Coates D. R. (Ed.), *Landslides*, Geological Society of America, Reviews in Engineering Geology, **3**, 29–56.

Netterberg, F. and Caiger, J. H. 1983. 'A geotechnical classification of calcretes and other pedocretes', in Wilson R. C. L. (Ed.), *Residual Deposits: Surface Related Weathering Processes and Materials*, Geological Society Special Publication **11**, Blackwell Scientific Publications, Oxford, 235–243.

Nicoletti, P. G. and Sorriso-Valvo, M. 1991. 'Geomorphic controls of the shape and mobility of rock avalanches', *Geological Society of America Bulletin*, **103**, 1365–1373.

Nicoletti, P. G., Parise, M. and Miccadei, E. 1993. 'The Scanno rock avalanche (Abruzzi, South-central Italy)', *Bollettino della Società Geologica Italiana*, **112**, 523–535.

Nonveiller, E. 1992. 'Vaiont slide – Influence of frictional heat on slip velocity', in Semenza, E. and Melidoro, G. (Eds), *Proceedings of the Meeting on the 1963 Vaiont landslide, Ferrara*, 187–197.

Parise, M. and Guzzi, R. 1992. *Volume and Shape of the Active and Inactive Parts of the Slumgullion Landslide, Hinsdale County, Colorado*, US Geological Survey, Open-File Report **92–216**, p. 29.

Perna, G. and Sauro, U. 1978. 'Atlante delle microforme da dissoluzione carsica superficiale del Trentino e del Veneto', *Memorie del Museo Tridentino di Scienze Naturali, nuova serie*, **22**, 1–176.

Postpischl, D. 1985. *Catalogo dei Terremoti Italiani dall'anno 1000 al 1980*, CNR – Progetto Finalizzato Geodinamica, Bologna, p. 239.

Read, S. A. L., Beetham, R. D. and Riley, P. B. 1992. 'Lake Waikaremoana barrier – A large landslide dam in New Zealand', *Proceedings of the 6th International Symposium on Landslides, Christchurch*, A. A. Balkema, Rotterdam, **2**, 1481–1487.

Rib, H. T. and Ta Liang, 1978. 'Recognition and identification', in Schuster, R. L. and Krizek, R. J. (Eds), *Landslides, Analysis and Control*, Transportation Research Board Special Report **176**, National Academy of Science, Washington, DC, 34–80.

Sassa, K. 1988. 'Special lecture: Geotechnical model for the motion of landslides, *Proceedings of the 5th International Symposium on Landslides, Lausanne*, A. A. Balkema, Rotterdam, **1**, 37–55.

Skempton, A. W. and Hutchinson, J. N. 1969. 'Stability of natural slopes and embankment foundations', *Proceedings of the 7th International Conference on Soil Mechanics and Foundation Engineering, Mexico*, State of the Art Volume, 291–240.

Varnes, D. J. 1978. 'Slope movements types and processes', in Schuster, R. L. and Krizek, R. J. (Eds), *Landslides, Analysis and Control*, Transportation Research Board Special Report **176**, National Academy of Science, Washington, DC, 11–33.

Voight, B. and Faust, C. 1982. 'Frictional heat and strength loss in some rapid landslides', *Géotechnique*, **32,** 43–54.
Völk, H. 1989. 'Die Bergsturzkatastrophe im Veltlin 1987', *Die Geowissenschaften*, 7(1), 1–9.
Voza, G. 1982. 'Le ville romane del Tellaro e di Patti in Sicilia e il problema dei rapporti con l'Africa', *Mitteilungen des Deutschen Archäologischen Instituts, Römische Abteilung*, Ergänzungsheft **25,** 202–209.